

Correlation effects in the density of states of annealed $\text{Ga}_{1-x}\text{Mn}_x\text{As}$

S. Russo and T.M. Klapwijk

Kavli Institute of Nanoscience, Delft University of Technology, The Netherlands

W. Schoch and W. Limmer

Dept. of Semiconductor Physics, University of Ulm, Germany

(Dated: November 10, 2018)

We report on an experimental study of low temperature tunnelling in hybrid NbTiN/GaMnAs structures. The conductance measurements display a \sqrt{V} dependence, consistent with the opening of a correlation gap (Δ_C) in the density of states of $\text{Ga}_{1-x}\text{Mn}_x\text{As}$. Our experiment shows that low temperature annealing is a direct empirical tool that modifies the correlation gap and thus the electron-electron interaction. Consistent with previous results on boron-doped silicon we find, as a function of voltage, a transition across the phase boundary delimiting the direct and exchange correlation regime.

PACS numbers: 75.50.Pp,73.40.Gk,71.30+h

The new class of ferromagnetic semiconductors $\text{Ga}_{1-x}\text{Mn}_x\text{As}$ is known¹ to display a metal-insulator transition (MIT) as function of Mn doping. In conventional doped semiconductors the MIT, which occurs as a function of carrier density, is widely studied and considered to be a prime example of a quantum phase transitions. It is understood that the spatial localization of charge carriers, which drives the MIT, reduces the ability of the system to screen charges, leading to a prominent role of the electron-electron interactions. The experimental trace of the Coulomb interactions between the electrons is the depletion of the single-particle Density of States (DOS) $N(E)$ at the Fermi energy^{2,3,4,5,6,7,8,9}. For a dirty three dimensional system it is found that $N(E) \sim \sqrt{E}$ in the metallic regime^{3,4}, whereas $N(E) \sim E^2$ in the insulating regime², recently observed in different localized systems^{5,6,7}, including magnetically doped materials⁸.

Recently, using conductance measurements across the metal-insulator-transition Lee⁹ constructed the phase diagram shown in Fig. 1a. At low enough temperatures, 10mK, the energy is controlled by the voltage at which the differential conductance is measured. For low energies, *i.e.* very close to the Fermi energy where the theory for the MIT is valid the system is a Coulomb gap insulator below the critical density and a correlated metal above the critical density. For higher energies a mixed state develops around the critical density, in which the density of states on both sides of the transition have a common functional dependence on energies masking the existence of a critical density. The “pure” state at low densities is the regime where exchange correlations describe the Coulomb interactions, whereas above the critical density the direct Coulomb interactions rule. At low energies the DOS is clearly distinct for metallic and insulating samples and the system is in the “pure” state. At high energies the insulating and metallic states are indistinguishable from DOS-measurements.

The new material system GaMnAs is for low Mn doping an insulator and the resistivity diverges for $T \rightarrow 0$,

indicating localization effects. In the metallic regime this (III,V)Mn is characterized by a decreasing resistivity which eventually saturates for $T \rightarrow 0$, although these resistivity values remain relatively high ($\sim 10^{-3} \Omega\text{cm}$, see Fig. 4(c)). Thus GaMnAs is a dirty metal where disorder plays a rather strong role. These strong electron-electron interaction effects the DOS of GaMnAs¹⁰ and might lead to the observation of the phase boundary cross-over from direct to exchange correlation at much higher temperatures than for Si:B.

Here we report the observation of the correlation gap in GaMnAs as measured with a tunnel contact between GaMnAs and the superconductor NbTiN. At the interface we have a Schottky barrier, which at low temperatures acts as a tunnel contact, allowing a direct measurement of the density of states. Superconducting leads are chosen, on top of unpatterned GaMnAs (inset Fig. 2), to ensure that the tunnel junction resistances are at least an order of magnitude larger than the sample resistance. The T-shape is chosen to minimize the effect of parallel conductance paths. With these samples we study systematically the evolution of the correlation energy (Δ_C) on the annealing time. We find experimentally that Δ_C decreases monotonously with annealing. This behavior suggests that with annealing the surface of the GaMnAs is driven away from the metallic towards the insulating state. Furthermore, measurements at bias voltage higher than Δ_C lead to the observation of a cross-over from the *direct* correlation regime to the *mixed* state behavior (as in Fig. 1b), consistent with previous results obtained on Si:B⁹.

The $\text{Ga}_{1-x}\text{Mn}_x\text{As}$ samples (Mn-content of 4.4%) are grown on (001) semi-insulating GaAs substrates by low temperature molecular-beam epitaxy (MBE) at 230°C. The GaMnAs epilayer (thickness of 40 nm, $T_{\text{Curie}} = 64\text{K}$) is patterned to hold two independent devices: a Hall bar and the T-shaped tunnel-contacts. The Hall bar ($200 \times 50 \mu\text{m}^2$, see inset of Fig. 3a) allows the characterization of the magnetic properties of GaMnAs. Electron Beam Lithography (EBL), Ar RF sputter cleaning

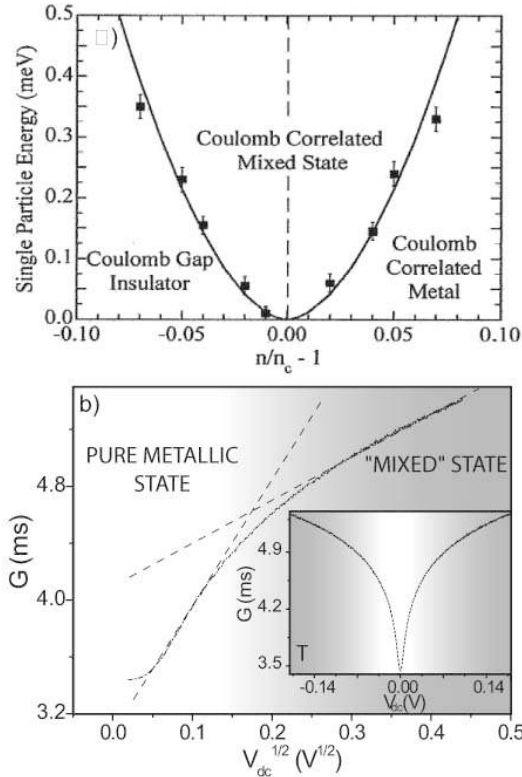


FIG. 1: a) Phase-diagram proposed by Lee⁹ to indicate the electron-correlated regimes at low energies and high energies as a function of carrier density. b) In the inset conductance *versus* voltage bias for our NbTiN/GaMnAs devices. Gray gradient in the background highlights the transition across the phase boundary delimiting direct and exchange correlation regime. At low bias the superconducting gap of the contact material causes a deviation.

and reactive sputtering are used to define the top NbTiN (thickness = 30 nm, superconducting transition temperature $T_C = 15$ K and superconducting gap $\Delta_S = 2$ mV). The contacts on the GaMnAs have a separation of 100 nm and a total area of $0.5 \times 1 \mu\text{m}^2$ (see Inset of Fig. 2). The tunnel-devices are used to measure the differential resistance.

In the standard tunneling model¹¹, the tunneling conductance $G(V, T) = \partial I / \partial V$ is the product of the density of states in the interacting material, $N_F(E)$, with the density of states of the superconductor, $N_S(E)$, convoluted with the Fermi-distributions. In view of the relevant energies we can ignore the thermal smearing. $N_S(E)$ is given by the standard BCS density of states as usually modified by a broadening parameter Γ ¹²: $N_S(E) = N(0) \text{Re}[(E - i\Gamma) / (\sqrt{(E - i\Gamma)^2 - \Delta_S^2})]$. The GaMnAs is described as dirty 3D metal system^{3,4}, thus $N_F(E) = N(0)(1 + \sqrt{(E)}/(\Delta_C))$. Δ_C is the correlation gap which represents the strength of the electron-electron interaction in the ferromagnetic semiconductor. In this tunneling description there are two free parameters, Γ and Δ_C , while the other parameters are known indepen-

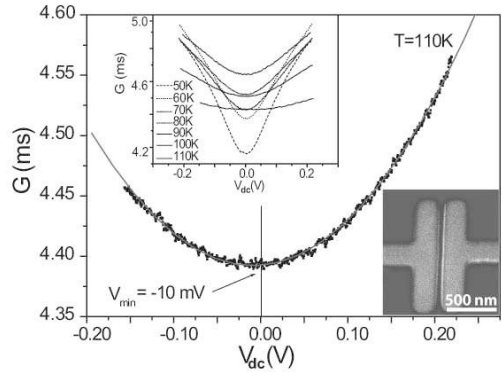


FIG. 2: Central inset: measurements at different temperatures of G *versus* V after annealing a device for 120 min and having a T_{Curie} of 96 K. Lower inset: a micrograph of one of the nano-fabricated S/F/S samples. The main figure shows a conductance measurement at $T = 110$ K. The full line is a best fit to the BDR model¹³, used to determine the barrier height.

dently.

For temperatures above the T_{Curie} the conductance displays a parabolic dependence on bias voltage¹⁰ (see Fig. 2). At lower temperatures deviations from the parabolic behavior occur (see inset in Fig. 2) which reflect, as we will show, the correlation gap. We focus now on the 2-probe conductance through the SFS device for $T > T_{\text{Curie}}$, Fig. 2. It is apparent that G clearly displays a parabolic dependence on bias voltage, which demonstrates that tunnelling is taking place, as described by Brinkman, Dynes and Rowell (BDR)¹³. The measured conductance for $T > T_{\text{Curie}}$ shows a slightly asymmetric shape and the occurrence of a minimum at a finite voltage bias ($V_{\min} = -10$ mV). These two features in the measurements are typical for the tunnel conductance in metal-insulator-metal junctions with different barrier heights at the interfaces.

In applying the BDR model to our data to estimate the barrier height at the S/F interface, we assume that the conduction in the GaMnAs is mainly due to the heavy holes with an effective mass of $0.462m_0$ ¹⁴. In addition we assume a thickness of the barrier at S/F of 10\AA ¹⁵. From fitting the curve of $G(V)$ to the BDR model, continuous line in Fig. 2, we find that the mean barrier height is $\bar{\varphi} = 0.33$ V. Furthermore the bias voltage at which the minimum conductance occurs ($V_{\min} = -10$ mV) gives a difference in barrier heights at the S/F interface of $\Delta\varphi = 16$ mV. Finally, we emphasize that the measured resistance of the two tunnel contacts in series is much higher than the resistance of the GaMnAs in between. These facts lead us to conclude that it is reasonable to assume that the measured conductance is a tunnel conductance.

Previous experiments have demonstrated that low temperature post growth annealing offers the possibility to change the ferromagnetic properties of GaMnAs¹⁷. Our samples are annealed in the same way, but performed on

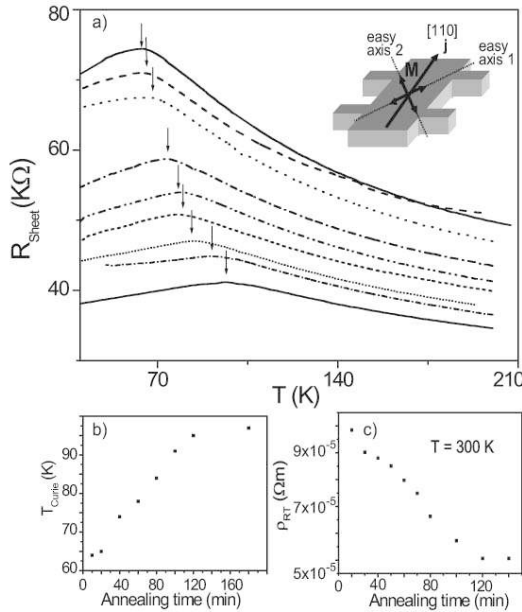


FIG. 3: a) Plot of the sheet resistance versus temperature for a GaMnAs Hall bar device, e.g. inset. Different curves are for different annealing times, from top to bottom: 0, 10, 20, 40, 60, 80, 100, 120, and 180 min. T_{Curie} is highlighted by the arrows. b) The T_{Curie} increases linearly with annealing time up to 120 min. and it remains unchanged for further annealing to 180min. c) The room temperature resistivity decreases as function of annealing time.

fully processed structure with the NbTiN on top of the GaMnAs. This leaves the interface unexposed to air. We do not observe any change in the critical current of the NbTiN, which excludes possible degradation of the superconductor. The annealing is performed at 200°C on a hot plate in air¹⁸ for a sequence of annealing times up to 180 min. In Fig. 3 we present measurements of the sheet resistance *versus* temperature performed on the Hall bar for different annealing times. The resistance displays a non monotonous dependence on temperature. It reaches a maximum at the Curie temperature¹ and eventually decreases, for $T < T_{\text{Curie}}$, as expected for metallic samples. From the graph of T_{Curie} *versus* annealing time (Fig. 3b) it is apparent that T_{Curie} increases¹⁹. It remains basically unchanged for further annealing to 180min. which is consistent with more extensive work presented by Stanciu *et al.*¹⁶. This enhancement of T_{Curie} has been usually traced back to a removal of compensating defects, and thus, to an increase of the hole concentration^{17,20}. In fact channeling Rutherford backscattering¹⁷ and Auger²⁰ experiments have shown that annealing at low temperature causes a migration of Mn interstitial defects towards the surface of GaMnAs. The fact that bulk ferromagnetic properties improve with low temperature annealing is also evident from the room temperature resistivity (ρ_{RT}), see Fig. 3c. ρ_{RT} decreases monotonously with annealing time, confirming that a reduction of defects and an increase of charge density takes place in GaMnAs¹⁸.

The 2-probe tunnel conductance measured at 4.2K is

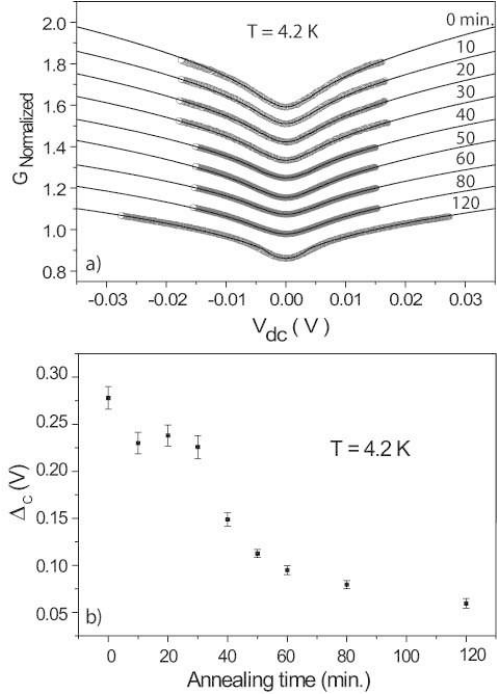


FIG. 4: a) 2-Probe tunnel conductance measurements for different low-temperature annealing times (shown for each graph). For increasing annealing time the non linear character of the curves at high bias is reduced. The solid lines are fits, leading to the correlation gap Δ_C . b) Δ_C decreases monotonously with annealing time.

shown in Fig. 4a. The measurements are normalized to the conductance value at 0.015V (arbitrarily chosen) and shifted for clarity. For $V < \Delta_{\text{NbTiN}}$ the superconducting state of the leads dominate the data. However for $V > \Delta_{\text{NbTiN}}$ correlation effects play the major role in transport and the measured conductance displays a non-linear character with the expected \sqrt{V} dependence on the bias voltage. This \sqrt{V} behavior indicates that the GaMnAs acts as a three dimensional dirty metal, with correlation effects parametrized with correlation gap Δ_C . We find experimentally that the non linear character of the conductance curves is progressively reduced as a function of increased annealing time. The continuous lines in Fig. 4a are the best fit to the tunneling model. Standard non-linear fitting is used with the parameters Δ_C and Γ , and minimization of the χ^2 merit function is carried out according to the Levenberg-Marquardt method. Good agreement between theory and experiments is found, and for each different annealing time the corresponding value of Δ_C is extracted (see Fig. 4b); the values found for Γ are $1 \pm 0.2 \text{ mV}$.

We observe that the interaction parameter in the as grown sample is $\Delta_C = 278 \text{ mV}$ ²¹ and it reduces to a smallest value of 59mV by annealing the sample for 120 minutes, see Fig. 4b. As shown in Fig. 3 annealing leads to an increase in T_{Curie} (from 64K to 97K) and a de-

crease in ρ_{RT} by 48 %, which suggests an improvement in the quality of material. However, the tunneling measurements lead to the conclusion that the correlation gap becomes smaller indicative of a system which is driven from the metallic regime to a more insulating regime. This behavior is consistent with the fact that with increasing annealing time a larger number of compensating defects reaches the surface, causing an increase in resistivity and a reduction of the correlation energy. Thus low temperature annealing, while improving the ferromagnetic properties of the bulk material (see Fig. 2), drives the surface of GaMnAs from the metallic towards the insulating state.

We now turn to the tunnel conductance measurements at higher bias voltage, higher than the correlation gap ($V_{bias} > \Delta_C$, e.g. inset Fig. 1b). We focus on a sample annealed for 120 minutes and $\Delta_C = 59$ mV. From Fig. 1b it is apparent that $G \sim \sqrt{V}$ over the entire bias range but with two different slopes, one at low energy and a less steep one at higher energy. The cross-over between these two regimes occurs at the bias corresponding to the correlation gap. Similar results have been presented by Lee⁹, although at much lower energies. Adopting the interpretation of Ref.⁹ we conclude that at low energies the GaMnAs is properly described as a dirty metal where correlation effects are manifested in a minimum in the DOS at the Fermi Energy. However, at high energies the \sqrt{V}

dependence stems from a mixture of direct and exchange correlations. At high energies GaMnAs displays a cross-over to the *mixed* state. The fact that the energy scale of the correlation gap in GaMnAs is much higher than in Si:B allowed the observation of this cross-over at modest temperatures.

In conclusion, we have studied correlation effects in the density of states of GaMnAs. Low temperature post-processing annealing is found to modify the electron-electron correlation in GaMnAs. Our experiments suggest that annealing acts in opposite ways on the bulk compared to the surface of GaMnAs: while improving the ferromagnetic properties of the bulk it drives the surface from the metallic state towards the insulating state. Hence, we find that annealing is a good external parameter which can be used to monitor continuously the evolution of the correlation gap when approaching the MIT at the surface of GaMnAs. Interestingly the tunnel conductance measurements display a cross-over from a low energy regime to an high energy regime allowing to track the phase boundary separating the pure metallic behavior from the *mixed* state, as found previously in Si:B by Lee⁹.

The authors acknowledge a useful discussion with S. Rogge. This work was financially supported by NWO/FOM and the Deutsche Forschungsgemeinschaft, DFG Li 988/4.

¹ F. Matsukura, H. Ohno, A. Shen and Y. Sugawara, Phys. Rev. B **57**, 2037(R) (1998).

² A.L. Efros and B.I. Shklovskii, J. Phys. C **8**, L49 (1975).

³ B.L. Altshuler and A.G. Aronov, Solid State Commun. **30**, 115 (1979).

⁴ W.L. McMillan, Phys. Rev. Lett. **24**, 2739 (1981).

⁵ J.G. Massey and M. Lee, Phys. Rev. Lett. **50**, 4266 (1995).

⁶ H.B. Chan, P.I. Glicofridis, R.c. Ashoori and M.R. Melloch, Phys. Rev. Lett. **79**, 2867 (1997).

⁷ E. Bielejec, J. Ruan and W. Wu, Phys. Rev. Lett. **87**, 036801 (2001).

⁸ W. Teizer, F. Hellman and R.C. Dynes, Phys. Rev. Lett. **85**, 848 (2000). L. Bokacheva, W. Teizer, F. Hellman, and R. C. Dynes, Phys. Rev. B **69**, 235111 (2004).

⁹ M. Lee, Phys. Rev. Lett. **93**, 256401 (2004).

¹⁰ S.H. Chun, S.J. Potashnik, K.C. Ku, P. Schiffer and N. Samarth, Phys. Rev. B **66** 100408(R) (2002).

¹¹ See, for example, E.L. Wolf, *Principles of Electron Tunneling Spectroscopy* (Oxford Univ. Press, Oxford, 1985).

¹² R.C. Dynes, V. Narayanamurti and J.P. Gorno, Phys. Rev. Lett. **41**, 1509 (1978).

¹³ W.F. Brinkman, R.C. Dynes and J.M. Rowell, Phys. Rev. B, **41** 1915 (1970).

¹⁴ T. Dietl, H. Ohno and F. Matsukura, Phys. Rev. B **63** 195205 (2001).

¹⁵ W. Mönch, *Semiconductor Surface and Interfaces*, Springer (2001).

¹⁶ V. Stanciu, O. Wilhelmsson, U. Bexell, M. Adell, J. Sadowski, J. Kanski, P. Warnicke, and P. Svendlidh, Phys. Rev. B **72**, 125324 (2005).

¹⁷ K.M. Yu, W. Walukiewicz, T. Wojtowicz, I. Kuryliszyn, X. Liu, Y. Sasaki and J.K. Furdyna, Phys. Rev. B **65**, 201303(R) (2002).

¹⁸ This particular annealing temperature was chosen because it results in a pronounced increase of T_C on our materials: see W. Limmer, A. Koeder, S. Frank, M. Glunk, W. Schoch, V. Avrutin, K. Zuern, R. Sauer and A. Waag, Physica E **21**, 970-974 (2004).

¹⁹ S. J. Potashnik, K.C. Ku, S.H. Chun, J.J. Berry, N. Samarth and P. Schiffer, Appl. Phys. Lett. **79**, 1495 (2001). K.W. Edmonds, K. Y. Wang, R.P. Campion, A.C. Neumann, N.R.S. Farley, B.L. Gallagher and C.T. Foxon, Appl. Phys. Lett. **81** 4991 (2002).

²⁰ K.W. Edmonds, P. Boguslawski, K. Y. Wang, R.P. Campion, S.N. Novikov, N.R.S. Farley, B.L. Gallagher, Phys. Rev. Lett. **92**, 037201 (2004).

²¹ Similar values of correlation energy where observed in Al granular films with resistivities comparable to our GaMnAs film: see G. Hertel, D.J. Bishop, E.G. Spencer, J.M. Rowell and R.C. Dynes, Phys. Rev. Lett. **50**, 743 (1983).